Revista Mexicana de Astronomía y Astrofísica, **58**, 73–82 (2022)

https://doi.org/10.22201/ia.01851101p.2022.58.01.06

FIRST LIGHT CURVE ANALYSIS OF THE MODERATE FILL-OUT CONTACT BINARY SYSTEMS TYC 2402-643-1, TYC 2703-1235-1 AND TYC 2913-2145-1

Carlo Barani[1], Francesco Acerbi[2], and Velimir Popov[3]

Received April 25 2021; accepted November 23 2021

ABSTRACT

We present the results of our study of the W Ursae Majoris eclipsing binary systems (EW) TYC 2402-643-1, TYC 2703-1235-1 and TYC 2913-2145-1 based on CCD observations obtained using Sloan *g'* and *i'* filters. The light curves were analysed using the latest version of the Wilson-Devinney code, and the obtained data were used to estimate the physical parameters of the systems. TYC 2402-643-1 and TYC 2913-2145-1, having mass ratio < 0.25, can be classified as Extreme Mass Ratio Binary (EMRBs) systems and belong to the A-subtype class of the EW. The third one, TYC 2703-1235-1, having mass ratio q about 3 ($1/q = 0.33$) belongs to W-subtype class of the EW. The absolute dimensions of the primaries and secondaries were estimated and investigated using different evolutionary diagrams.The parameters of the progenitors of the components of the systems were calculated and the results are consistent with the determination of the subtypes.

RESUMEN

Presentamos los resultados de nuestro estudio de tres binarias eclipsantes de tipo W Ursae Majoris: TYC 2402-643-1, TYC 2703-1235-1 y TYC 2913-2145-1, basado en observaciones CCD con los filtros Sloan *g'* e *i'*. Se analizaron las curvas de luz con la última versión del código Wilson-Devinney, y con los datos obtenidos se estimaron los parámetros físicos de los sistemas. TYC 2402-643-1 y TYC 2913-2145-1, con un cociente de masas de < 0.25, pueden ser clasificadas como binarias con cociente de masas extremo (EMRBs) y pertenecen al subtipo A de las EW. TYC 2703-1235-1, con un cociente de masas q de aproximadamente 3 ($1/q = 0.33$) pertenece al subtipo W de las EW. Se investigaron las dimensiones absolutas de las primarias y de las secundarias con distintos diagramas evolutivos. Se calcularon los parámetros de las progenitoras de las componentes de los sistemas. Los resultados concuerdan con las determinaciones de los subtipos.

Key Words: binaries: eclipsing — stars: fundamental parameters — stars: individual: TYC 2402-643-1, TYC 2703-1235-1, TYC 2913-2145-1

1. INTRODUCTION

The eclipsing binary star TYC 2402-643-1 (NSVS 6868895 = GSC 02402-00643 = UCAC4 635-024089) was proposed as a variable star in the list provided by Gettel et al. (2006) which suggested a period of variability of 0.399579 days.

Based on the four values of the new times of minima (ToM's), listed in Table 1, we propose the new ephemeris as:

$$\text{HJD(MinI)} = 2458865.3253(5) + 0.3992342(2) \times \text{E}. \quad (1)$$

TYC 2703-1235-1 (NSVS 8702136 = GSC 02703-01235 = UCAC4 604-123844) was found to be a variable star by Woźniak et al. (2004) from the Northern Sky Variability Survey.

The first period was indicated by J. S. Shaw and collaborators in their online list (https://www.

[1]Via Molinetto 35, 26845 Triulza di Codogno (LO), Italy.
[2]Via Zoncada 51, 26845 Codogno (LO), Italy.
[3]Department of Physics and Astronomy, Shumen University, Shumen, Bulgaria.

TABLE 1

CCD TIMES OF MINIMA FOR TYC 2402-643-1

HJD	Epoch$_{(1)}$	O−C$_{(1)}$	Error	Source
2458865.3249	0.0	0.0001	0.0021	This paper
2458865.5256	0.5	0.0010	0.0029	This paper
2458866.3232	2.5	-0.0006	0.0028	This paper
2458866.5232	3.0	-0.0004	0.0025	This paper

TABLE 2

CCD TIMES OF MINIMA FOR TYC 2703-1235-1

HJD	Epoch$_{(2)}$	O−C$_{(2)}$	Error	Source
2455799.4988	-8366.0	0.0020	0.0005	OEJV 160
2455800.4776	-8363.5	-0.0020	0.0010	OEJV 160
2459088.4634	0.0	0.0000	0.0034	This paper
2459089.4463	2.5	0.0001	0.0009	This paper
2459090.4289	5.0	-0.0001	0.0012	This paper

TABLE 3

CCD TIMES OF MINIMA FOR TYC 2913-2145-1

HJD	Epoch$_{(3)}$	O−C$_{(3)}$	Error	Source
2458867.4786	-5.5	0.0000	0.0052	This paper
2458870.4821	0.0	0.0000	0.0036	This paper

physast.uga.edu/~jss/nsvs/) as $P = 0.393128$ days and the type of variability was suggested as the W UMa system. Using two ToM's as obtained from literature Hoňkova et al. (2013) and three ToM's as observed by us (Table 2) we can propose a new ephemeris as follows:

$$\text{HJD (MinI)} = 2459088.4634(9) + 0.3931349(3) \times \text{E}. \quad (2)$$

TYC 2913-2145-1 also identified STARE aur0 1201 = GSC 02913-02145 = UCAC4 654-032034, was suggested as a variable, with a period of 0.54634 days, during the observations of the STellar Astrophysics and Research on Exoplanets (STARE) operating in the Canary Islands, Spain (http://www.hao.ucar.edu/research/stare/lc_database.html). The proposed variability was EB type.

During our observations we obtained two ToM's (Table 3) and the new ephemeris:

$$\text{HJD (MinI)} = 2458870.4821(3) + 0.5460860(2) \times \text{E}. \quad (3)$$

2. OBSERVATIONS AND DATA REDUCTION

The preliminary available information about the targets was taken from the AAVSO Variable Star Index database (VSX) and is presented in Table 4.

To investigate the absolute parameters, the eclipsing binary stars TYC 2402-643-1, TYC 2703-1235-1 and TYC 2913-2145-1 have been observed in 2020 with the 30-cm Ritchey Chretien Astrograph located into the *IRIDA South* dome of the NAO Rozhen - Bulgaria.

The astrograph was equipped with a focal reducer to work at f/5 and a CCD camera ATIK 4000M (2048 × 2048 pixels, 7.4 μm/pixel, pixel-scale of the optical system of 1.04 arcsec/pixel and a field of view of 35 × 35 arcmin).

The photometric observations were carried out with Sloan type filters in the *g', i'* bands and the log of CCD photometric observations is presented in Table 5.

The standard sequence (de-biasing, dark frame subtraction and flat-fielding) was applied for photometric data reduction by the software AIP4WIN2.0 Berry & Burnell (2006). The aperture ensemble photometry was carried out with the automatic photometry tool LesvePhotometry[4] de Ponthire (2010).

The color transformation was applied along with the previously estimated transformation coefficients of the optical system. To obtain the magnitudes in the respective color bands for the comparison and check stars we used the catalogue APASS DR9 Henden et al. (2015) (Table 6).

3. PHOTOMETRIC SOLUTIONS WITH THE W-D METHOD

No published photometric solutions have been found for all three systems. The latest version of the Wison-Devinney code, (Wilson & Devinney 1971, Wilson 1990, Wilson & van Hamme 2015) was used to perform a simultaneous analysis of the available light curves. The effective temperatures determined in different ways are shown in Table 7 where T_{g-i} is determined by the measured index $(g' - i')$ at quadrature while T^{der}_{g-i} is determined after dereddening, both by means of the relations from Covey et al. (2007); T_G is the Gaia DR2 temperature from Gaia Collaboration (Brown et al. 2018); T^{der}_{J-K} is determined by the 2MASS index $(J-K)$ from Skrutskie et al. (2006) while T^{der}_{B-V} is determined by the APASS DR10 index $(B - V)$, both after dereddening and by means of the relations from Pecaut & Mamajek (2013); T_{Lamost} are taken from the LAMOST DR5

[4] www.dppobservatory.net.

TABLE 4

PARAMETERS OF THE TARGETS FROM THE VSX DATABASE

Target	RA(2000)	Dec(2000)	Period, d	Mag.	Ampl.	Reference
TYC 2402-643-1	05:18:58.08	+36:58:05.96	0.399579	11.373(R1)	0.442	Gettel et al. (2006)
TYC 2703-1235-1	21:21:40.47	+30:36:07.02	0.393128	11.94(R1)	0.75	Hoffman et al. (2009)
TYC 2913-2145-1	05:21:42.98	+40:41:00.71	0.54634	10.61(R)	0.40	Brown & Charbonneau (2000)

TABLE 5

LOG OF PHOTOMETRIC OBSERVATIONS

Target	UT Date [yyyymmdd]	Exposures (g', i') [s]	Number (g', i')	Mean error (g', i') [mag]
TYC 2402-643-1	2020 Jan 16	30, 90	237, 237	0.011, 0.009
	2020 Jan 17	30, 90	204, 204	0.009, 0.008
TYC 2703-1235-1	2020 Aug 26	60, 90	106, 106	0.008, 0.009
	2020 Aug 27	60, 90	167, 167	0.004, 0.005
	2020 Aug 28	60, 90	86, 86	0.004, 0.005
TYC 2913-2145-1	2020 Jan 18	30, 90	240, 240	0.007, 0.006
	2020 Jan 20	30, 90	98, 98	0.009, 0.009
	2020 Jan 21	30, 90	223, 223	0.006, 0.006
	2020 Jan 23	30, 90	113, 113	0.006, 0.007

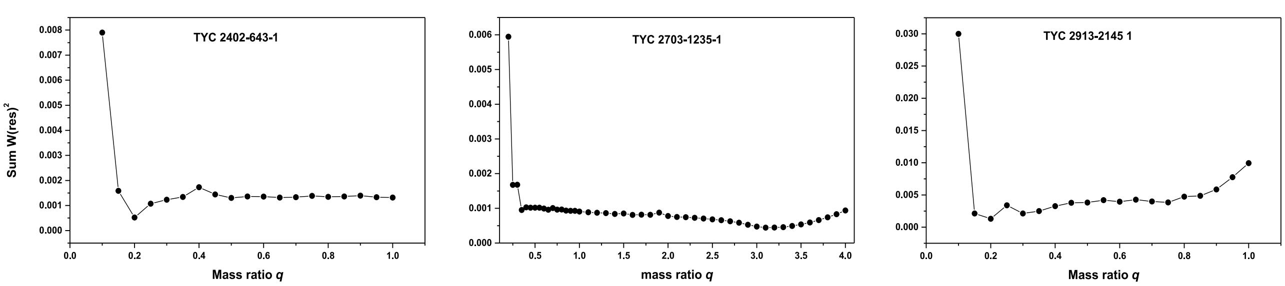

Fig. 1. The relation $\Sigma(res)^2$ versus mass ratio q in Mode 3 for the three systems in the WD code.

catalog (Luo et al. 2019). The last column indicates the mean effective temperatures of the targets T_m, adopted here for the procedures of the light curves solutions.

The shape of the light curves of these systems is similar to the most frequent light curve shapes of the W UMa type binary stars, so the classical Mode 3 (overcontact configuration) of the W-D code was used.

The q-search procedure was used, leaving as free parameters the temperature of the secondary components T_2, the inclination i of the systems, the non-dimensional surface potentials ($\Omega_{1=2}$) and the monochromatic luminosities of the primary components L_1. Other parameters such as g_2, A_2, L_2, x_2 and y_2 are not free but fixed to their theoretical values.

As soon as the $\Sigma(res)^2$ showed a minimum value we also added the value of the mass-ratio q to the set of the free parameters and ran a new W-D working session that only stopped when the corrections to the parameters became smaller than their probable errors (Figure 1).

The mass-ratio converged to a value of $q = 0.210$ for TYC 2402-643-1, $q = 3.05$ ($1/q = 0.327$) for TYC 2703-1235-1 and $q = 0.193$ for TYC 2913-2145-1 in the final solution. The value of the mass ratios for the first and the third systems corresponds to a transit at the primary minima inherent to the A-subtype contact binaries, while for

TABLE 6

MAGNITUDES OF THE COMPARISON AND CHECK STARS

Label	Star ID	RA(2000)	Dec(2000)	g'	i'
Target	TYC 2402-643-1	05 18 58.10	+36 58 05.2	11.349	10.797
Chk	UCAC4 636-024573	05 19 01.87	37 02 53.48	12.973	11.620
C1	UCAC4 636-024658	05 19 21.61	37 02 27.18	13.639	12.624
C2	UCAC4 636-024637	05 19 15.80	37 01 23.13	13.006	12.393
C3	UCAC4 635-024132	05 19 08.76	36 58 06.84	12.222	11.689
C4	UCAC4 636-024521	05 18 48.57	37 05 08.70	12.560	11.966
C5	UCAC4 636-024485	05 18 39.27	37 06 07.67	11.680	11.514
C6	UCAC4 635-024236	05 19 35.14	36 50 25.01	11.455	10.924
Target	TYC 2703-1235-1	21 21 40.52	+30 36 08.1	11.745	11.043
Chk	UCAC4 604-123798	21 21 23.20	30 36 01.70	12.897	11.945
C1	UCAC4 604-123970	21 22 24.04	30 45 07.66	12.889	11.076
C2	UCAC4 604-123988	21 22 28.49	30 42 26.83	13.124	12.607
C3	UCAC4 604-123848	21 21 41.68	30 39 27.15	12.409	12.245
C4	UCAC4 604-123814	21 21 28.51	30 41 03.43	11.854	10.543
C5	UCAC4 603-128892	21 21 45.45	30 33 40.65	12.735	12.606
C6	UCAC4 604-123956	21 22 19.14	30 36 55.52	12.170	10.988
C7	UCAC4 604-123756	21 21 04.98	30 37 11.64	12.252	12.052
Target	TYC 2913-2145-1	05 21 42.90	+40 40 58.0	10.972	10.580
Chk	UCAC4 654-031899	05 20 56.36	40 38 49.86	12.606	11.747
C1	UCAC4 654-032144	05 22 23.34	40 41 51.84	12.089	11.489
C2	UCAC4 654-031940	05 21 10.50	40 47 17.45	12.483	11.898
C3	UCAC4 654-032070	05 21 54.82	40 42 32.33	12.351	11.873
C4	UCAC4 653-032388	05 21 46.72	40 32 29.57	11.919	11.528
C5	UCAC4 655-033047	05 21 32.40	40 48 41.47	10.969	11.063
C6	UCAC4 654-032142	05 22 22.81	40 47 31.99	10.229	10.138

TABLE 7

TARGET TEMPERATURES

Target	T_{g-i}	T_G	T_{Lamost}	T_m
TYC 2402-643-1	5899	6429	6511	6280
Target	T^{der}_{g-i}	T^{der}_{J-K}	T^{der}_{B-V}	T_m
TYC 2703-1235-1	6180	5884	5736	5930
Target	T_{g-i}	T_G	T^{der}_{J-K}	T_m
TYC 2913-2145-1	6254	6694	6530	6470

TYC 2703-1235-1 the value corresponds to an occultation at primary minima, a typical W-subtype contact binary in the Binnendijk (1965) classification.

The light curve of TYC 2703-1235-1 shows asymmetries between the two maxima with Max II higher than Max I by 0.02 mag in the *g'* filter, the well known inverse O'Connell effect (O'Connell 1951), while in the *i'* filter this effect is not detectable. To justify this asymmetry, a small 25° hot spot has been placed on the surface of the primary component of the system.

The fact that the presence of a hot spot tends to be less noticeable at longer wavelengths is already known and it is an indication of a wavelength-dependent hot spot activity, probably due to an impact from a mass transfer between the components.

It is well known that in the Wilson-Devinney program the errors of the adjustable parameters are unrealistically small. The problem of unrealistically small errors is not intrinsic to the WD method nor related only to parameter correlations. In fact the WD code provides the "probable" errors, which are derived by the differential correction routine and are related to the standard errors of the linearized least-squares algorithm, and the errors can be used as a measure of the uncertainties only for normal distributions of the photometric errors.

Many strategies are possible to obtain an independent estimate of the uncertainties in a light curve analysis. One of these is to approach the problem

TABLE 8

VALUES OF THE FITTED PARAMETERS

Target	q	i [°]	$\Omega_{1,2}$	T_1 [K]	T_2 [K]	θ [°]	φ [°]	γ [°]	Ts/T$_*$
TYC 2402-643-1	0.210(6)	86.79(43)	2.2216(12)	6280(fxd)	6088(43)	-	-	-	-
TYC 2703-1235-1	3.054(30)	81.77(44)	6.5507(29)	5930(fxd)	5725(86)	91.2(9)	20.7(1.1)	25.1(7)	1.05(2)
TYC 2913-2145-1	0.194(5)	88.61(58)	2.1870(23)	6470(fxd)	5740(86)	-	-	-	-

TABLE 9

CALCULATED PARAMETERS

Target	r_1	r_2	f	l_1	l_2	$\Sigma(res)^2$
TYC 2402-643-1	0.530(10)	0.266(2)	0.273	0.798(23)	0.177(3)	0.000469
TYC 2703-1235-1	0.299(2)	0.491(2)	0.238	0.286(34)	0.665(5)	0.000455
TYC 2913-2145-1	0.535(2)	0.258(2)	0.221	0.861(23)	0.122(1)	0.001232

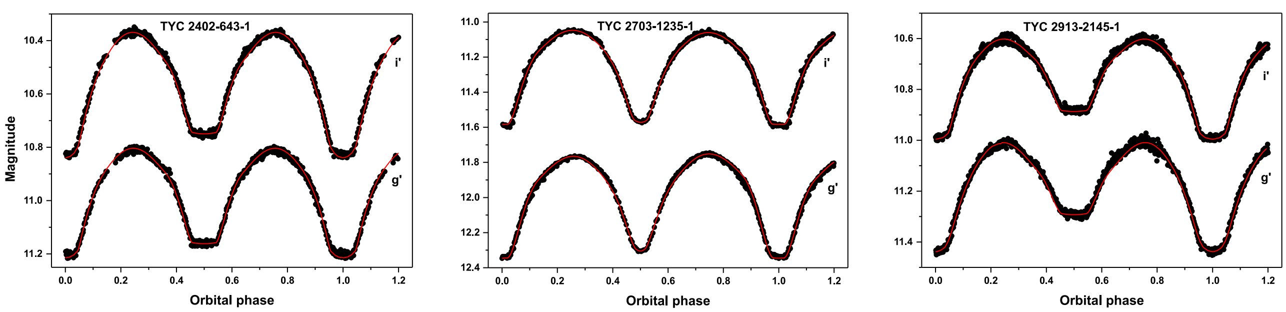

Fig. 2. CCD light curves of the systems. The points are the original CCD observations and the full lines are the theoretical fits with the surface spot contribution. The color figure can be viewed online.

through the bootstrap technique (Efron & Tibshirani 1986, Esmer et al. 2021), that allows to estimate parameter confidence levels of least squares solutions.

For this purpose we have generated many different data samples of free parameters(i, $\Omega_{1,2}$, T_2, l_1 and q) by random resampling with repetitions (bootstrapping), performing the minimization procedure for each sample and deriving confidence intervals from the resulting distribution of parameters.

The full set of parameters from our solutions is listed in Tables 8 and 9. The results of our modeling and the obtained fitted curves are shown in Figure 2, while graphic representations of the three systems are shown in Figure 3, using the Binary Maker 3.0 software (Bradstreet & Steelman 2002).

4. ESTIMATE OF THE ABSOLUTE RELATIVE ELEMENTS

Since no spectroscopic measurements of the orbital elements are available at present, the absolute parameters of the systems cannot be determined directly. Therefore, these results should be considered "relative" rather than "absolute" parameters and regarded as preliminary. The low galactic latitude of the systems implies that interstellar reddening E(B-V) may be large. Therefore, we have preferred to use a statistical method for the estimation of the absolute elements instead of a method based on the Gaia distance.

The empirically three-dimensional correlations from Gazeas (2009) $M(P,q)$, $R(P,q)$, given below,

$$\log M_1 = 0.725(59)\log P - 0.076(32)\log q + 0.365(32),$$

$$\log M_2 = 0.725(59)\log P + 0.924(33)\log q + 0.365(32),$$

$$\log R_1 = 0.930(27)\log P - 0.141(14)\log q + 0.434(14),$$

$$\log R_2 = 0.930(29)\log P + 0.287(15)\log q + 0.434(16),$$

and the Stefan-Boltzmann law

$$L_{1,2} = R_{1,2}^2 * (T_{1,2}/T_\odot)^4,$$

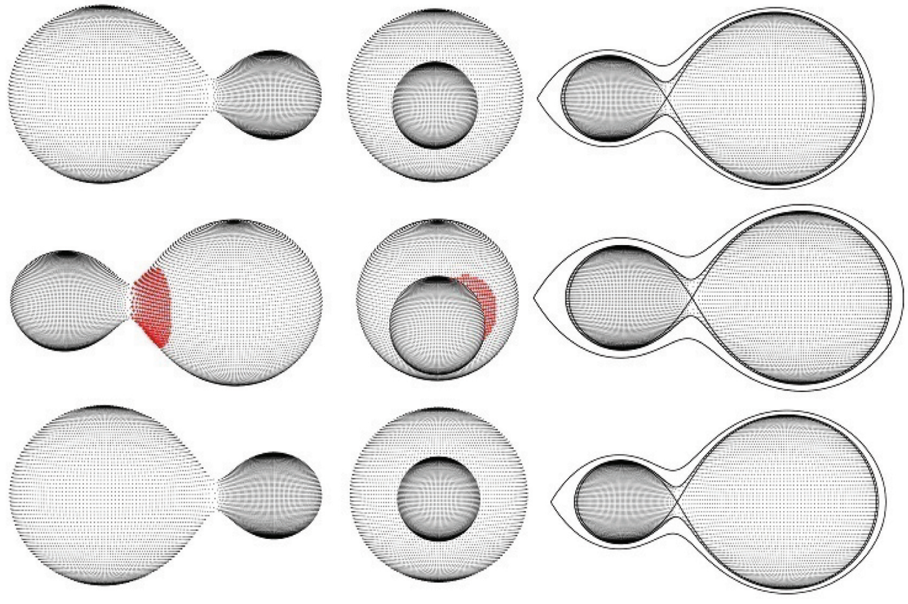

Fig. 3. Graphic representation of TYC 2402-643-1 (top), TYC 2703-1235-1 (middle) and TYC 2913-2145-1 (bottom) according to our solution, at quadrature (left) and at the primary minimum (center). Right: the configuration of the components of the systems in the orbital plane is shown. The color figure can be viewed online.

TABLE 10

RELATIVE PARAMETERS

Target	L_1 $[L_\odot]$	L_2 $[L_\odot]$	R_1 $[R_\odot]$	R_2 $[R_\odot]$	a $[R_\odot]$	M_1 $[M_\odot]$	M_2 $[M_\odot]$	Sp.type
TYC 2402-643-1	2.91(76)	0.68(20)	1.44(7)	0.74(5)	2.68(12)	1.34(17)	0.28(4)	F7V+F9V
TYC 2703-1235-1	0.66(20)	1.99(52)	0.83(6)	1.33(7)	2.70(12)	0.42(6)	1.28(17)	G0V+G3V
TYC 2913-2145-1	6.00(1.6)	0.91(28)	1.95(10)	0.97(7)	3.55(16)	1.69(22)	0.33(5)	F5V+G3V

Note: Spectral types are according to Pecaut & Mamajek (2013).

allowed us to have a preliminary estimate of the relative parameters of the systems under study. It is important to note that the empirical law does not give the full solution but an approximation of their physical parameters, as the single quantities are affected by errors of 13% and 14% for M_1 and M_2, 5% and 7% for R_1 and R_2.

In the article by Gazeas (2009) it is stated that the empirical laws relating to the 3D domain are affected by an error of less than 5%. In order to verify whether this statement is a under or overestimated value, we have applied the above relations to the catalog of contact binaries reported in the article by Gazeas & Stępień (2008) thus calculating masses, radii and luminosity of all systems. Comparing the difference between the calculated parameters and those reported in the catalog, we found that the RMS of the residuals is much higher than 5%. This procedure has therefore allowed us to obtain more realistic values of the uncertainties of the estimated values of the absolute elements reported in Table 10.

We used the estimated relative elements of the systems as reported in Table 10 to investigate the evolutionary states of our targets by comparing the location of their components on the main sequence (MS) diagrams expressed as $\log T$-$\log L$, $\log M$-$\log L$, $\log M$-$\log R$, and $\log M$-$\log T$. We built the isochrone tracks for the zero age main sequence (ZAMS) and the terminal age main sequence (TAMS) according to the PARSEC models (Bressan et al. 2012), as shown in Figure 4. As the PARSEC models extend up to 30 Gyr we limited the TAMS evolutionary tracks to stars with masses larger than $0.7M_\odot$.

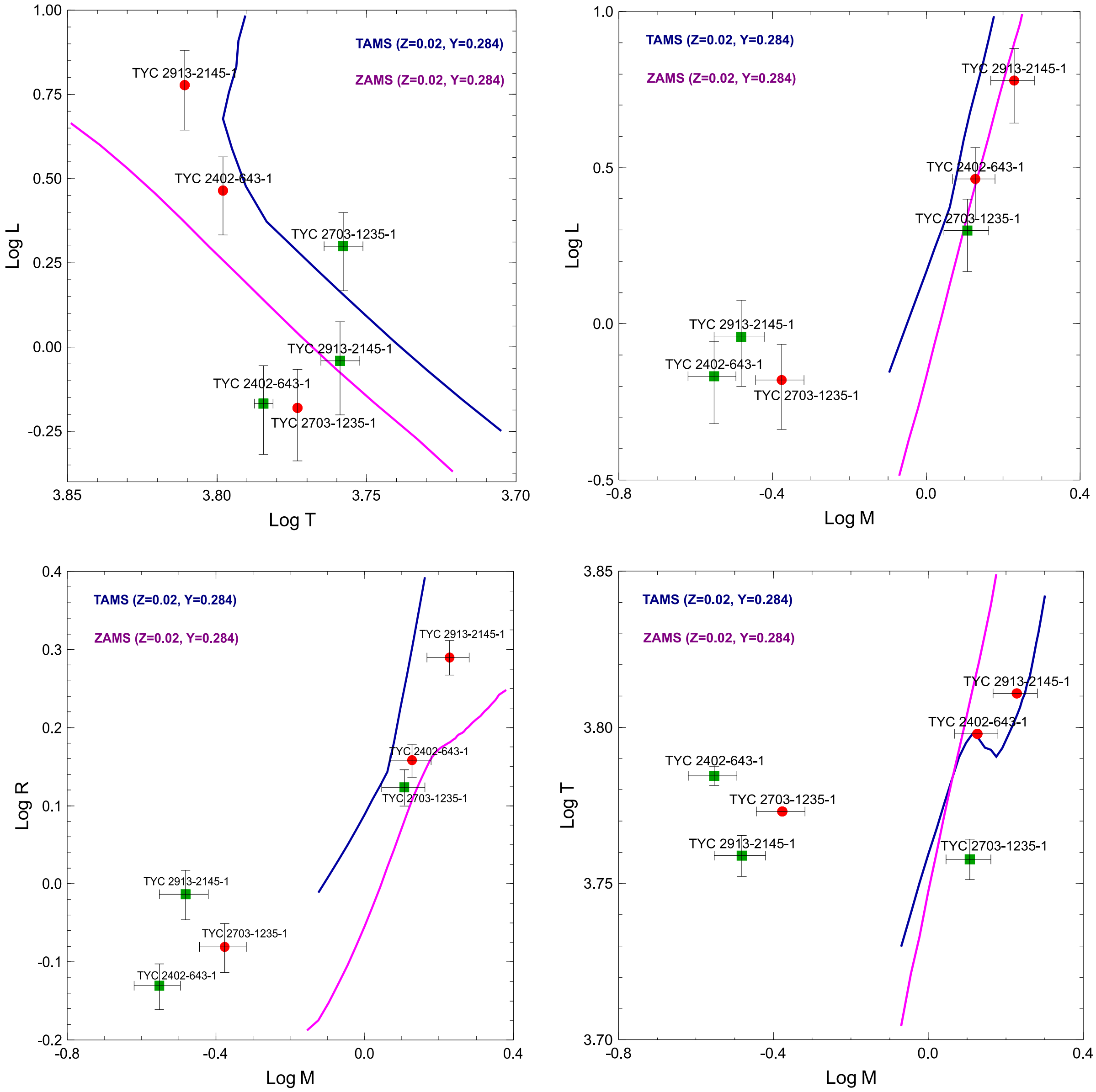

Fig. 4. Properties of our targets shown against evolutionary tracks of $\log T - \log L$, $\log M - \log L$, $\log M - \log R$, and $\log M - \log T$ (Bressan et al. 2012). The primaries are marked with red circles and the secondaries with green squares. The color figure can be viewed online.

The correlations between the absolute parameters of our targets (W UMa stars) differ from the correlations between the parameters of the stars belonging to MS. The evolutionary states of the binary components of our targets are similar. The more massive components are near the ZAMS, meaning that they are little evolved stars, while the less massive components are located above the TAMS, implying that they have evolved away from the main sequence. These results are due to the mass and energy exchange between the binary components and their internal evolutionary transformations.

The three targets do not differ from the general cases of the EW type stars, where the less massive components of the binary systems have a luminosity larger than that of a main sequence star with the same mass and radius, (Yakut & Eggleton 2005, Yildiz & Doğan 2013). For the W subtype this phenomenon can be due to the energy transfer from the primary to the secondary star that changes the sec-

TABLE 11

PARAMETERS OF THE PROGENITORS OF THE SYSTEMS

Target	Subtype	M_{1i} $[M_\odot]$	M_{2i} $[M_\odot]$	a_{fof} $[R_\odot]$	P_{fof} [Days]
TYC 2402-643-1	A	0.82	1.84	5.43	0.8996
TYC 2703-1235-1	W	2.18	0.39	5.39	0.8569
TYC 2913-2145-1	A	1.16	1.92	5.94	0.9575

ondary and makes it over-sized and over-luminous for its mass (Webbink 2003, Li et al. 2008). The secondary components of the A-subtype are thought to have evolved from initially more massive stars (Zhang et al. 2020).

5. FROM DETACHED TO CONTACT PHASE

The formation of the W UMa type contact binaries is a complex process in which different mechanisms are combined.

Yildiz & Doğan (2013) developed a method for the computation of the initial masses of contact binaries. Their main assumption is that the mass transfer starts near or after the TAMS phase of the initially massive component, which is the progenitor of the currently less massive components. They discovered that binary systems with an initial mass larger than $1.8 \pm 0.1\ M_\odot$ become A-subtype, while systems with initial masses smaller than this become W-subtype.

By applying their method to our systems we derived the masses of the progenitors of the systems M_{2i} and M_{1i} with the semi-major axis a_{fof} and the orbital periods P_{fof} at the time of the first overflow (i.e fof).

These parameters are computed from equations from Yildiz & Doğan (2013) as developed by Kriwattanawong & Kriwattanawong (2019) and are reported in our Table 11.

6. CONCLUSIONS

We have derived, for the first time, a photometric solution for the eclipsing binary systems TYC 2402-643-1, TYC 2703-1235-1 and TYC 2913-2145-1.

TYC 2402-643-1 and TYC 2913-2145-1 are found to be A-type contact binaries and, having mass ratios < 0.25, can be classified as extreme mass ratio binary systems (EMRBs) (Samec et al. 2015). The discovery of binaries with extremely low mass ratios as our targets and other similar, such as USNO-B1.0 1452-0049820 and ASAS J102556+2049.3 from Kjurkchieva et al. (2018a) and NSVS 2569022 with $q = 0.077$ and of some others as were pointed out in Table 3 of Kjurkchieva et al. (2018b) provoke future theoretical investigations to establish the lower mass ratio limit of the W UMa type stars.

TYC 2703-1235-1 was found to be a W-subtype with a mass ratio of $q = 3.054$ ($q_{inv} = 0.327$) and a shallow fill-out parameter of $f = 22.1\%$. These characteristics agree with those of most W-subtype contact systems.

Our systems have high orbital inclination, between 81 and 88 degrees, displaying total eclipses, so the photometric parameters obtained here are reliable (Terrell & Wilson 2005).

W UMa systems generally show an almost equal temperature for the components, and this is the case for two of the three systems. In contrast, TYC 2913-2145-1 is in a relatively poor thermal contact with $\Delta T = 730$K. The relatively large difference in temperature and the shallow fill-out value could indicate that TYC 2913-2145-1 may be at a key evolutionary stage, as predicted by the thermal relaxation oscillation theory (TRO) (Lucy 1967, Lucy & Wilson 1979, Flannery 1976, Robertson & Eggleton 1977, Eggleton 1996, Qian & Ma 2001, Yakut & Eggleton 2005, Li et al. 2005, and Li et al. 2008).

From our observed ToM's as well as from those obtained from the literature we cannot say much about the period variation of the systems, but we used the data in our analysis for refining the ephemeris.

Following the work of Qian et al. (2020) it is possible to see that the position of TYC 2913-2145-1 in the period-temperature correlation graph is just on the outer edge of the lower boundary, confirming that it is at the beginning of the evolutionary stage of contact binary evolution (Figure 5), as assumed by us due to both its relatively large temperature difference and the low value of contact between the components.

The other two systems show a good thermal contact with difference in temperatures between the components of a couple of hundred K, and are well inside the boundaries for normal EW; they will approach the final evolutionary stage of the contact binary evolution (Figure 5).

Absolute parameters were estimated for the components. The overluminosity of the secondaries in the W UMa systems can be due to the energy transfer from the primary to the secondary for the

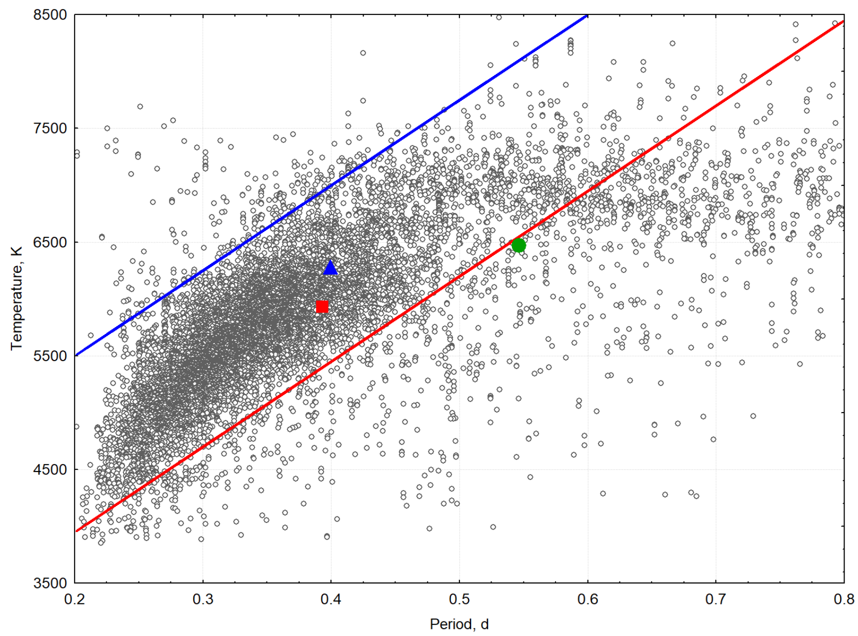

Fig. 5. Correlation between orbital period and temperature based on parameters of 8510 contact binaries from Qian et al. (2020). The position of TYC 2402-643-1 is marked in blue, the one of TYC 2703-1235-1 in red and the one of TYC 2913-2145-1 in green. The red and blue lines are the boundaries of normal EWs. Systems near the red border are marginal contact systems, while those close to the blue border are deep contact ones. The color figure can be viewed online.

W-subtype, and to the evolution of the secondary component from an initial more massive star of A-subtype.

The study of Yildiz & Doğan (2013) shows that the W UMa binary systems with an initial mass of the secondary component of the system ($M2_i$, the actual primary component) larger than $1.8\pm0.1 M_\odot$ become A subtype, while the systems with initial masses smaller than this become W subtype.

By applying the method to our systems we are able to estimate the absolute relative parameters of the detached system, the progenitor of the contact system, as shown in Table 11. We found that the initial mass of the secondary component of the two A-subtypes would be greater than 1.8 solar masses, while for the W-subtype system it would be smaller than that value, as predicted.

The results show that the angular momentum of the three systems has decreased; consequently, the orbital period and the semi-major axis have decreased too. To verify the reliability of our results we used the relationship between masses and ratios as specified in Qian (2001). We found that our systems do not deviate from these correlations.

The research was supported in part by project D01-383/20 of the Scientific Fund of the Bulgarian Ministry of Education and Science. The research was made with the support of the private IRIDA OBSERVATORY.[5] This work has used data from the European Space Agency (ESA) mission GAIA, processed by the GAIA Data Processing and Analysis Consortium (DPAC). Funding for the DPAC has been provided by national institutions, in particular the institutions participating in the GAIA Multilateral Agreement. This research has used the SIMBAD database, operated at CDS, Strasbourg, France, NASA Astrophysics Data System Abstract Service. We are thankful to Svetla Potter for the English language corrections. We would like to thank the anonymous referee for all her/his very useful comments and corrections which have improved the quality of this paper.

REFERENCES

Berry, R. & Burnell, J. 2006, The Handbook of Astronomical Image Processing with AIP4WIN2 software, (Willmann-Bell. Inc. WEB.)

Binnendijk, L. 1965, VeBam 27, The Position of Variable Stars in the Hertzsprung-Rusell Diagram, 36

Bradstreet, D. H. & Steelman, D. P. 2002, AAS, 201, 7502

[5]http://www.irida-observatory.org.

Bressan, A., Marigo, P., Girardi, L., et al. 2012, MNRAS, 427, 127, https://doi.org/10.1111/j.1365-2966.2012.21948.x
Brown T. M. & Charbonneau, D. 2000, ASPC 219, Disks, Planetesimals, and Planets, ed. F. Garzón, C. Eiroa, D. de Winter, and T. J. Mahoney (ASP), 584
Covey, K. R., Ivezić, Ž, Schlegel, D., et al. 2007, AJ, 134, 2398, https://doi.org/10.1086/522052
de Ponthire, P. 2010, LESVEPHOTOMETRY, automatic photometry software (http://www.dppobservatory.net)
Efron, B. & Tibshirani, R., 1986, StaSc, 1, 54, https://doi.org/10.1214/ss/1177013815
Eggleton, P. P. 1996, ASPC 90, The origins, evolution, and destinies of binary stars in clusters, ed. E. F. Milone & J. -C. Mermilliod (San Francisco, CA: ASP), 257
Esmer, B. M., Baştürk, Ö., Hinse, T. C., Selam, S. O., & Correia, A. C. M. 2021, A&A, 648, A85, https://doi.org/10.1051/0004-6361/202038640
Flannery, B. P. 1976, ApJ, 205, 217, https://doi.org/10.1086/154266
Gaia Collaboration, Brown, A. G. A., Vallenari, A., et. al. 2018, A&A, 616, 1, https://doi.org/10.1051/0004-6361/201833051
Gazeas, K. D. 2009, CoAst, 159, 129,
Gazeas, K. D. & Stępień, K. 2008, MNRAS, 390, 1577, https://doi.org/10.1111/j.1365-2966.2008.13844.x
Gettel, S. J., Geske, M. T., & McKay, T. A. 2006, AJ, 131, 621, https://doi.org/10.1086/498016
Henden, A. A., Levine, S., Terrell, D., & Welch, D. L. 2015, AAS, 225, 336.16
Hoffman, D. I., Harrison, T. E., & McNamara, B. J. 2009, AJ, 138, 466, https://doi.org/10.1088/0004-6256/138/2/466
Hoňková, K., Juryšek, J., Lehký, M., et al. 2013, OEJV, 160, 1
Kjurkchieva, D. P., Popov, V. A., & Petrov, N. I. 2018, AJ, 156, 77, https://doi.org/10.3847/1538-3881/aace5e
_________. 2018, RAA, 18, 129, https://doi.org/10.1088/1674-4527/18/10/129
Kriwattanawong, W. & Kriwattanawong, K. 2019, RAA, 19, 143, https://doi.org/10.1088/1674-4527/19/10/143
Li, L., Han, Z., & Zhang, F. 2005, MNRAS, 360, 272, https://doi.org/10.1111/j.1365-2966.2005.09024.x
Li, L., Zhang, F., Han, Z., Jiang, D., & Jiang, T. 2008, MNRAS, 387, 97, https://doi.org/10.1111/j.1365-2966.2008.12736.x
Lucy, L. B. 1967, ZA, 65, 89
Lucy, L. B. & Wilson, R. E. 1979, ApJ, 231, 502
Luo, A.-L., Zhao, Y.-H., Zhao, G., et al. 2019, yCat, 5164, 0
O'Connell, D. J. K. 1951, PRCO, 2, 85
Pecaut, M. J. & Mamajek, E. E. 2013, ApJS, 208, 9, https://doi.org/10.1088/0067-0049/208/1/9
Qian, S.-B. 2001, MNRAS, 328, 914, https://doi.org/10.1046/j.1365-8711.2001.04921.x
Qian, S.-B. & Ma, Y. 2001, PASP, 113, 754
Qian, S.-B., Zhu, L.-Y., L. Liang, et al. 2020, RAA, 20, 163
Robertson, J. A. & Eggleton, P. P. 1977, MNRAS, 179, 359, https://doi.org/10.1093/mnras/179.3.359
Samec, R. G., Benkendorf, B., Dignan, J. B., et al. 2015, AJ, 149, 146, https://doi.org/10.1088/0004-6256/149/4/146
Skrutskie, M. F., Cutri, R. M., Stiening, R., et al. 2006, AJ, 131, 1163, https://doi.org/10.1086/498708
Terrell, D. & Wilson, R. E. 2005, Ap&SS, 296, 221, https://doi.org/10.1007/s10509-005-4449-4
Webbink, R. F. 2003, ASPC 293, 3D Stellar Evolution, ed. S. Turcotte, S., S. C. Keller, & R. M. Cavallo (ASP), 76
Wilson, R. E. & Devinney, E. J. 1971, ApJ, 166, 605, https://doi.org/10.1086/150986
Wilson, R. E. 1990, ApJ, 356, 613, https://doi.org/10.1086/168867
Wilson, R. E. & van Hamme, W. 2015, Computing binary stars observables, ftp.astro.ufl.edu, directory pub/wilson/lcdc2015
Woźniak, P. R., Vestrand, W. T., Akerlof, C. W., et al. 2004, AJ, 127, 2436, https://doi.org/10.1086/382719
Yakut, K. & Eggleton, P. P. 2005, ApJ, 629, 1055, https://doi.org/10.1086/431300
Yildiz, M. & Doğan, T. 2013, MNRAS, 430, 2029, https://doi.org/10.1093/mnras/stt028
Zhang, X.-D., Qian, S.-B., & Liao, W. P. 2020, MNRAS, 492, 4112, https://doi.org/10.1093/mnras/staa079
Zhang, X.-D. & Qian, S.-B. 2020, MNRAS, 497, 3493, https://doi.org/10.1093/mnras/staa2166

Francesco Acerbi: Via Zoncada 51, 26845 Codogno (LO), Italy (acerbifr@tin.it).
Carlo Barani: Via Molinetto 35, 26845 Triulza di Codogno (LO), Italy (cvbarani@alice.it).
Velimir Popov: Department of Physics and Astronomy, Shumen University, 115 Universitetska str., 9700 Shumen, Bulgaria (velimir.popov@elateobservatory.com, v.popov@shu.bg).